Online supplement to

Geometry of the Turkey-Arabia and Africa-Arabia plate boundaries in the latest Miocene to Mid-Pliocene: the role of the Malatya-Ovacık Fault Zone in eastern Turkey

by

Rob Westaway, Tuncer Demir, and Ali Seyrek

Local evidence related to the kinematics of the MOFZ

This supplement discusses local evidence related to the kinematics of the Malatya-Ovacık fault zone (MOFZ). It summarizes previous interpretations of this structure and notes a number of difficulties with these, then presents new evidence regarding the relationship of this fault zone to its regional context. Aspects of this new interpretation are used in the development of the regional kinematic model in the main text.

As envisaged by Westaway and Arger (1996, 2001), the MOFZ consists of two principal fault segments, the ~100 km long NNE-trending Malatya Fault that links end-on at its NNE end into the ~140 km long ENE-trending Ovacık Fault (Fig. 2 in main text). Both the Malatya and Ovacik faults were first recognized long ago (e.g., by Arpat and Şaroğlu, 1975). As noted in the main text, the principal evidence for the Malatya Fault was a major linear escarpment along the WNW margin of the Malatya Basin. Evidence for the Ovacık Fault is provided, first, by the ENE-trending lineation of the Ovacık valley at the SSE margin of the ~3400 m high Munzur mountain range. Second, beyond the WSW end of the Ovacık valley, several rivers, including the Euphrates (Fig. 2 in the main text), are offset left-laterally by concordant distances of ~8 km.

Regional context

The Malatya region (see Figs. 1, 2 in the main text) is located in eastern Anatolia, ~50 km north of the suture of the former Southern Neotethys Ocean. This brief summary of their history is based on published information, including Aktaş and Robertson (1984), Bingöl (1984), Michard et al. (1984), Perinçek and Kozlu (1984), Yazgan (1984), and Hempton (1985). This ocean basin formerly connected the ocean basins in the eastern Mediterranean Sea and Indian Ocean, separating the Arabian Platform from Anatolia. It began to close in the Late Cretaceous (~90 Ma) at the start of convergence between the African and Eurasian plates, closure being accommodated by northward subduction beneath Anatolia. Ophiolite obduction occurred in the latest Cretaceous (Maastrichtian; ~70 Ma), followed by relative stability in the Palaeocene, when AF-EU relative motion was minimal. Closure by northward subduction resumed in the Eocene, lasting until the Middle Eocene (Lutetian) by which point no ocean basin remained at the longitude of the Malatya region and the continental crust of the Arabian Platform was juxtaposed against that of Anatolia. Subsequent convergence between Africa/Arabia and Eurasia, accommodated by shortening of the continental crust, lasted until the Late Cenozoic strike-slip fault systems began to develop in the latest Miocene. Most of eastern Anatolia was below sea-level in the Early Cenozoic, but subsequent regional surface uplift led to the subaerial emergence of the Malatya region and its surroundings to the east and south in the late Early Miocene.

The oldest rocks that crop out in the study region comprise the Malatya and Keban metamorphics, derived from carbonate-rich marine sediments of Late Palaeozoic - Early Mesozoic age, now metamorphosed to marble and calcschist. These are overthrust by rocks related to the Late Cretaceous subduction, usually known as the Yüksekova Complex or Elazığ Complex, comprising extrusive and intrusive igneous rocks, subduction-related sediments, and ophiolite. The succession of younger sediments and volcanics related to (and immediately post-dating) the brief Eocene phase of subduction is generally known as the Maden Complex (e.g., Aktaş and Robertson, 1984). There is little evidence of sedimentation in the region during most of the Oligocene, but Early Miocene marine limestone is extensive, assigned a range of local names (as in Figs S1 and S2). This study will not address the evidence pre-dating the Late Cenozoic; recent detailed accounts of the magmatism, sedimentation, and structural development associated with the Late Cretaceous and Eocene phases of subduction include work by Cronin et al. (2000), Rizaoğlu et al. (2006), and Robertson et al. (2007).

The Westaway and Arger (2001) scheme

As noted above, Westaway and Arger (2001) envisaged the MOFZ as a predecessor of the EAFZ. From geological and geomorphological evidence they estimated that the MOFZ accommodated 29 km of relative motion between the Turkish and Arabian plates. The geomorphological evidence used included the ~25 km length of the Ovacık valley (Fig. 2 in the main text), which was interpreted as a pull-apart basin on the Ovacık Fault. This estimate of the total slip on the Ovacık Fault is much greater than the largest of the river offsets along it; Westaway and Arger (2001) attributed this to river capture accompanying drainage translocation (cf. Westaway et al., 2006b). The geological evidence included a number of outcrop boundaries that Westaway and Arger (2001) used as piercing points. However (as Westaway and Arger, 2001, indeed made clear), due to the political situation in eastern Turkey in the mid 1990s, when this work was done, it was impossible to visit many such localities in the field; data thus had to be taken from published maps without ground-truthing.

In this scheme, the Malatya Fault was envisaged as a left-lateral transform fault, the difference in altitude of the land surface across it being attributed to sediment-loading of the crust on its ESE side, beneath the Malatya Basin. Conversely, Westaway and Arger (2001) envisaged the Ovacık Fault and the adjoining Munzur mountain range as forming a transpressive structure, with deformation beting partitioned between left-lateral slip on the Ovacık Fault and distributed crustal shortening in its surroundings, causing localised surface uplift wthin the Munzur mountain range.

This scheme did not contradict any information that was known at the time when it was developed. It is now called into question by the seismic reflection evidence provided by Kaymakçı et al. (2006), which suggests instead a transtensional geometry for the Malatya Fault (see below). In addition, following the improvement in the political situation in eastern Turkey since 1999 it has become possible to inspect in the field many localities that were previously inaccessible. Such fieldwork has established that some of the previously published mapping evidence used by Westaway and Arger (2001) to infer piercing points for measuring slip on the MOFZ is incorrect (see below), invalidating the basis for inferring large magnitude (up to ~30 km) left-lateral slip on the MOFZ.

The Kaymakçı et al. (2006) scheme

On the contrary, Kaymakçı et al. (2006) envisaged the Malatya and Ovacık faults as separate structures, with independent histories. Based on their seismic reflection profiling results and analysis of remote sensing data and of microstructural kinematic indicators in the field, they inferred a three-phase history for the Malatya Fault. In their view its first phase of slip occurred in the Early and Middle Miocene and was associated with WNW-ESE extension, leading to the accumulation of much of the Malatya Basin succession in the hanging-wall of this fault. During their second phase, spanning the Late Miocene and Early Pliocene, the region experienced N-S compression, which caused the reactivation of the Malatya Fault in a left-lateral sense and also caused N-S crustal shortening on adjacent structures, such as the Aydnlar thrust (Fig. 2 in the main text). In their view, during the third phase, which has lasted since the Late Pliocene, the region has remained under N-S compression but the Malatya Fault has not slipped significantly in any sense. Furthermore, in the view of Kaymakçı et al. (2006), the Malatya Fault continues northward past the western end of the Ovacık Fault, before dying out; it does not link end-on into the latter structure.

Likewise, although Kaymakçı et al. (2006) considered the Ovacık Fault as not directly connected to the Malatya Fault, they envisaged it as having first developed as a normal fault in the Early-Middle Miocene, followed by reactivation in a compressive sense, associated with left-lateral slip, starting in the Late Miocene.

Major difficulties with this Kaymakçı et al. (2006) scheme include fhe lack of reasons offered for why the region experienced extension in the Early-Middle Miocene followed by compression starting in the Late Miocene. Furthermore, the suggestion that the Malatya and Ovacık faults experienced similar histories of reactivation but were not kinematically linked seems arbitrary.

New Observations

Given the difficulties noted above, we have re-examined much of the MOFZ and its surroundings, to elucidate the role of this structure. This work has reached the following conclusions. First, the land surface west of the Malatya Basin is gently folded as an anticline, the fold axis being located ~15 km west of the Malatya Fault (see Fig. 2 in the main text). This gentle folding is revealed by lateral variations in the altitudes of Late Cenozoic marine and lacustrine sediments and of the overlying Kepezdağı basalt. It is supported by the geomorphology of the adjacent Tohma river gorge, which has cut down into Cretaceous rocks near this anticline axis (Fig. S1a), then passes downstream, up-section, into the overlying Cenozoic succession (e.g., Ayan and Bulut, 1964).

Figure S1 here: Field photos west of the Malatya Basin

Second, the disposition of the sediments and basalt in this area indicates that they pre-date the folding. The shapes of the basalt outcrops indicate that basalt flowed NE, towards the centre of the Malatya Basin, not WNW or ESE as would be required by the modern topographic gradients oriented away from the aforementioned anticline axis. The typical altitude of the base of the basalt increases ESE from ~1500 m near Balaban (Akkuş (1971), to ~2000 m at Aygörmez Dağı (Fig. S1b), near the fold axis, then declines to ~1900 m at Yığılıçakıl Tepe, east of this axis. The westernmost limit of the Early Miocene marine limestone (known locally as the Tahtalı Tepe Formation) is also near Balaban, where this deposit is only ~30 m thick and reaches ~1500 m a.s.l. (Akkuş, 1971). Its surface altitude increases eastward to ~1800 m near Güneşli (Fig. S1c) then decreases to ~1700 m beneath Yığılıçakıl Tepe, east of the fold axis. Pockets of younger lacustrine sediment, mapped as "Late Miocene terrestrial deposits" or "Neogene" by Baykal (1961), cover much of the the land surface east of the fold axis, at altitudes that increase westward to ~1900 m, and are also present farther west (west of the fold axis) around Güneşli, at up to ~1850 m a.s.l., and around Kolköy (see Fig. 2 in the main text for locations). We can confirm the presence of such a deposit, locally ~50 m thick, at Güneşli (at [CB 90369 49898]). Apparently similar deposits, more than ~200 m thick, reaching up to ~2000 m a.s.l., are also present between the Early Miocene marine limestone and the Kepezdağı basalt at Aygörmez Dağı (Fig. S1b).

Third, this disposition of sediments indicates that the western 'escarpment' of the Malatya Basin, between the Malatya Fault and the anticline axis, is an ESE-sloping dip slope. Kaymakçı et al. (2006) proposed instead that this escarpment steps down via a number of normal fault offsets, but we found no evidence of that, nor did Westaway and Arger (2001). The Malatya Basin is thus a syncline, bounded to the WNW by this dip slope. The geometry of its ESE part, on the other side of the Malatya Fault, is well illustrated by the seismic sections presented by Kaymakçı et al. (2006); each unit of sediment typically dips WNW and also thickens WNW, towards the Malatya Fault.

Fourth, the geometry of the Malatya Basin, with the Malatya Fault located axially beneath the thickest sediment, could in principle indicate either a sag basin, fortuitously located over a transform fault, or it could indicate a transtensional basin. The disposition of sediment and basalt suggests to us that the lacustrine basin first developed as a sag basin, extending westward at least as far as Güneşli, then at a later stage the ancient zone of weakness beneath the basin was reactivated transtensionally, causing the development of the fold axis to the west of the basin and resulting in subsequent sedimentation being more strongly localized about the Malatya Fault.

Figure S2 here: Malatya Basin stratigraphic column

Figure S3 here: Malatya Basin cross-section

Fifth, the chronology of the Malatya Basin succession is disputed, as summarised in Fig. S2 caption. We consider two forms of evidence to be potentially significant. Notably, Kaymakçı et al. (2006) mentioned (without giving details) evidence of the ancestral mouse *Progonomys* sp. at their site 35, at [DC 41583 77639], near Karababa (formerly called Mamaar or Mamahar; Fig. 2 in the main text). Based on their co-ordinates and the mapping of the area by Önal (1997), we infer this site to be located as shown in Fig. S3, near the base of the Parçikan Formation. According to Agusti et al. (2001), the first appearance of *Progonomys cathalai* is in mammal zone MN10, which spans 9.7-8.7 Ma. On this basis, this sediment can be no older than early Late Miocene, making it younger than the Middle Miocene age determined for the Parçikan Formation by Önal (1995, 1997) using pollen. Furthermore, deposition of the coarse fluvial conglomerate of the Beyler Deresi Formation (Fig. S4a), the youngest part of this stacked sequence (Fig. S2), evidently required an environment conducive to a high rate of erosion (in adjoining upland areas, such as the Malatya Mountains; Fig. 2 in the main text) and sediment transport. Pervasive vegetation cover will prevent such high rates of erosion and sediment transport. By analogy with adjoining regions (e.g., western Turkey and Bulgaria; Westaway et al., 2006b; Westaway, 2006), it is expected that such vegetation cover was present until, at the earliest, the end of the Mid-Pliocene climatic optimum. We thus consider it unlikely that an environment consistent with deposition of the Beyler Deresi Formation could have existed during or before this time. We thus infer that this sediment probably post-dates this time, suggesting an age for it in the range ~3-2 Ma.

Figure S4 here: Malatya Basin photos

Sixth, in the vicinity of Küseyin (Figs S2, S3, S4b), the Malatya Basin succession has experienced deformation due to slip on a north-dipping reverse fault, known as the Aydınlar Thrust. Kaymakçı et al. (2006) proposed that this reverse faulting was synkinematic with slip on the Malatya Fault and also synkinematic with deposition of the younger part of the Malatya Basin succession. We see no basis for the former assertion and consider the latter assertion to be problematic, as the younger part of the basin succession is not found in the vicinity of this fault, making it impossible to establish the relative chronology on this basis. Farther east, escarpments thought to be related to other young reverse faults are also evident, such as the Piran Fault north of Baskil and the Harput Fault north of Elazığ (see Fig. 2 in the main text). Activity of the former structure is suggested by the depths of fluvial incision in its uplifted hanging wall (e.g., Tonbul, 1987); activity of the latter is suggested by the higher altitude of Pliocene lacustrine deposits, of the Karabakır Formation in its hanging-wall; these reach >1200 m a.s.l north of the fault but <1100 m a.s.l. south of it (e.g., Tonbul, 1987; Demir et al., 2004). Each of these instances of reverse faulting thus appears to be synkinematic with the EAFZ and thus younger than the MOFZ. However, to create the observed amounts of displacement, their slip rates need be no more than tenths of a mm a^{-1}; they would thus not be detectable by geodetic surveys (e.g., McClusky et al., 2000) that indicate no significant active deformation within the Turkish plate. We thus see no necessity to kinematically link this minor compressive deformation to the slip on the MOFZ (contra Kaymakçı et al., 2006).

Figure S5 here: Ovacık Fault photos

Finally, we have re-examined the evidence for the sense and amount of slip on the Ovacık Fault. Arpat and Şaroğlu (1975) first interpreted this as a normal fault, with downthrow to the SSE, the Munzur mountains forming its uplifted footwall. Having now visited this locality in the field (Fig. S5a), we are impressed at the resemblence between this structure and many other major normal faults elsewhere. We thus now accept that the Ovacık Fault has accommodated both normal (down to the SSE) and left-lateral slip, not pure left-lateral slip as Westaway and Arger (2001) inferred. Most of the evidence indicators for the total slip on the Ovacık Fault proposed by Westaway and Arger (2001) depend on it being a pure left-lateral fault, and can thus no longer be used. Potentially the most significant of the indicators remaining after this exclusion is that provided by the apparent offset of basaltic-andesite lavas between the vicinity of Arapkir on the Turkish plate side of the MOFZ and Şahinler on its Arabian side (* symbols in Fig. 2 in the main text), an offset distance that Westaway and Arger (2001) measured as 27.5 km. The presence of lava flows in the Arapkir area, part of the Yamadağ volcanism, is well established (e.g., Arger et al., 2000). Unfortunately, for reasons already stated, Westaway and Arger (2001) could only base their association of this volcanism with the Şahinler area from published mapping, by Baykal (1961). However, we found no lava in this area (around [DD 77194 37513]); instead, we found outcrop of hard, dark grey limestone, part of the Keban Group, which - we conclude - must have been mistaken for lava in the previous mapping. There is evidently no basis for any left-lateral offset on the MOFZ of the magnitude estimated by Westaway and Arger (2001). Furthermore, adjoining the Şahinler area, between Başpınar and Dutluca, is the reach of the River Euphrates that has become offset left-laterally by the Ovacık Fault by ~8 km (Fig 2 in the main text; Fig. S5b). Since the river began to be offset in this area it has incised into the adjoining land surface by more than ~400 m (see detailed discussion by Westaway and Arger, 2001). There is no evidence at either end of this offset reach for any geomorphological evidence of capture or diversion of the Euphrates, in contrast with other localities on strike-slip faults elsewhere in Turkey (cf. Westaway et al., 2006). We thus conclude (contra Westaway and Arger, 2001) that this river offset marks the total slip on the Ovacık Fault.

Additional references (not cited in the main text)

Agusti, J., Cabrera, L., Garces, M., Krijgsman, W., Oms, O., Pares, J.M., 2001. A calibrated mammal scale for the Neogene of western Europe: state of the art. Earth-Science Reviews 52, 247-260.

Akkuş, M.F., 1971. Geologic and stratigraphic investigation of the Darende-Balaban Basin (Malatya, ESE Turkey). MTA Dergisi, 76, 1-54.

Aktaş, G., Robertson, A.H.F., 1984. The Maden complex, SE Turkey: Evolution of a Neotethyan active margin. In: Dixon, J.E., Robertson, A.H.F. (Eds.), The Geological Evolution of the eastern Mediterranean. Geol. Soc. London Spec. Publ. 17, 375-402.

Arger, J., Mitchell, J., Westaway, R. 2000. Neogene and Quaternary volcanism of south-eastern Turkey. In: Bozkurt, E., Winchester, J.A., Piper, J.D.A. (Eds.), Tectonics and Magmatism of Turkey and the Surrounding Area. Geological Society, London, Special Publication 173, 459-487.

Asutay, H.J., 1988. Geological map of the Malatya-H27 quadrangle, 1:100,000 scale, and accompanying 12 page explanatory booklet. General Directorate of Mineral Research and Exploration, Ankara.

Ayan, T., Bulut, C., 1964. General geology of the area defined by the polygone Balaban-Yazıhan-Kurşunlu-Levent (Vilayet Malatya). MTA Dergisi, 62, 60-73.

Bingöl, A.F., 1984. Geology of the Elazığ area in the Eastern Taurus region. In: Tekeli, O., Göncüoğlu, M.C. (Eds.), Geology of the Taurus Belt, Proceedings of the 1983 Ankara Symposium. General Directorate of Mineral Research and Exploration, Ankara, p. 209-216.

Cronin, B.T., Hartley, A.J., Çelik, H., Hurst, A., Türkmen, I., Kerey, E., 2000. Equilibrum profile development in graded deep-water slopes: Eocene, Eastern Turkey. J. Geol. Soc., London, 157, 943-955.

Demir, T., Yeşilnacar, İ., Westaway, R., 2004. River terrace sequences in Turkey: sources of evidence for lateral variations in regional uplift. Proceedings of the Geologists' Association 115, 289-311.

Hempton, M.R., 1985. Structure and deformation history of the Bitlis suture near Lake Hazar, southeastern Turkey. Geol. Soc. Am. Bull., 96, 233-343.

Herece, E., Akay, E., Küçümen, Ö, Sarıaslan, M., 1992. Elazığ, Sivrice, Palu dolayının jeolojisi. Report no. 9634 (unpublished), General Directorate of Mineral Research and Exploration, Ankara.

Huntington, E., 1902. The valley of the upper Euphrates River and its people. Bulletin of the American Geographical Society 34, 301-318 and 384-393.
Kerey, İ.E., Türkmen, I. 1991. Sedimentological aspects of Palu formation (Plio-Quaternary), the east of Elazığ, Turkey. Bulletin of the Geological Society of Turkey 34, 21-26 (in Turkish with English summary).
McClusky, S., and 27 others, 2000. Global Positioning System constraints on plate kinematics and dynamics in the eastern Mediterranean and Caucasus. Journal of Geophysical Research 105, 5695-5719.
Michard, A., Whitechurch, H., Ricou, L.E., Montigny, R., Yazgan, E., 1984. Tauric subduction (Malatya - Elazığ provinces) and its bearing on tectonics of the Tethyan realm in Turkey. In: Dixon, J.E., Robertson, A.H.F. (Eds), The Geological Evolution of the eastern Mediterranean. Geol. Soc. London Spec. Publ. 17, 362-373.
Rizaoğlu, T., Parlak, O., Hoeck, V., İşler, F., 2006. Nature and significance of Late Cretaceous ophiolitic rocks and their relation to the Baskil granitic intrusions of the Elazığ region, SE Turkey. In: Robertson, A.H.F.; Mountrakis, D., eds, Tectonic development of the eastern Mediterranean region. Geological Society, London, Special Publications, 260, 327-350.
Robertson, A.H.F., Parlak, O., Rizaoğlu, T., Ünlügenç, Ü, İnan, N., Taslı, K., Ustaömer, T., 2007. Tectonic evolution of the South Tethyan ocean: evidence from the Eastern Taurus Mountains (Elazığ region, SE Turkey). In: Rees, A.C., Butler, R.W.H., Graham, R.H., eds, Deformation of the Continental Crust: The Legacy of Mike Coward. Geological Society, London, Special Publications, 272, 231-270.
Tonbul, S., 1987. Elazığ batusin genel jeomorphologie özellikleri ve gelisimi (General geomorphology to the west of Elazığ: aspects and development), Jeomorphologie Dergisi (Geomorphology Bulletin) 15, 37-52.
Westaway, R., Guillou, H., Yurtmen, S., Beck, A., Bridgland, D., Demir, T., Scaillet, S., Rowbotham, G., 2006b. Late Cenozoic uplift of western Turkey: Improved dating and numerical modelling of the Gediz river terrace staircase and the Kula Quaternary volcanic field. Global and Planetary Change, 51, 131-171.
Yazgan, E., 1984. Geodynamic evolution of the Eastern Taurus region. In: Tekeli, O., Göncüoğlu, M.C. (Eds.), Geology of the Taurus Belt, Proceedings of the 1983 Ankara Symposium. General Directorate of Mineral Research and Exploration, Ankara, p. 199-208.

Figure captions

Figure S1. Views illustrating the disposition of the Kepezdağı basalt.in relation to the underlyimg sediments, west of the Malatya Basin. **(a)** View NNW from [CC 98090 57836], ~1.5 km N of Kolköy, looking across the Tohma valley (the river being locally just under 900 m a.s.l., having incised down into Cretaceous rocks) to the basalt-capped summit flat of Göktepe, 1844 m a.s.l. and ~12 km away (at [CC 956 694]). Note the gentle westward tilting of this summit flat, at the western end of which the basalt is banked against older sediment. The major escarpment in the valley side is in the Middle Eocene limestone of the Asartepe Formation. The overlying Early Miocene limestone of the Tahtalı Tepe Formation forms another escarpment at a higher level, but the thinness of this deposit means that this is niot clearly visible at such a great distance. **(b)** Montaged photograph showing the view between WNW and NNW from [DC 04390 48277], at Develi (~1450 m a.s.l.) on the main toad from Malatya to Kayseri and Ankara. The skyline is formed in what remains of one of the largest flow units assigned to the Kepezdağı basalt, labelled Ay in Fig. 2 in the main text. This caps the summits of, from left to right, Aygörmez Dağ ([CC 994 510]; 2015 m a.s.l.), Huktepe ([DC 017 525]; 1950 m a.s.l.), and Yığılıçakıl Tepe ([CC 028 524]; 1927 m a.s.l.). The basalt overlies unlithified (?) Middle Miocene and younger lacustrine sdiments and lithified Early Miocene marine limestone, above lithified Middle Eocene limestone, which Akkuş (1971) called the the Tahtalı Tepe Formation. **(c)** View eastward from [CC 90866 50500], ~500 m NE of the village of Güneşli (formerly known as Akpınar) looking across the valley of the River Ebeler (or Dıpsız), the far skyline being the basalt-capped summit of Aygörmez Dağ (the opposite side of it to that visible in (a)), ~8 km away. In the foreground, and in the middle distance on the opposite side of the Ebeler valley, the upper part of the Early Miocene marine limestone (the Tahtalı Tepe Formation) is evident, at an altitude of ~1800 m a.s.l.. Above it, covered in basalt talus, is other sediment, not locally well-exposed, that is discussed in the text. Capping that (outside the field of view) is the Güneşli flow unit of the Kepezdağı basalt.

Figure S2. Schematic stratigraphic column (using standard notation for lithologies) for the stacked sequence of the southern Malatya Basin, based on Fig. 2 of Önal (1995) with additional information from Önal (1997). Thicknesses indicated refer to type localities. In the central Malatya Basin, Önal (1997) defined only the Boyaca Formation as overlying the Parçikan Foirmation, this being evidently a lateral equivalent of the Şeyhler Formation (Fig. S3). The top of the Beyler Deresi Formation has been incised by modern rivers, such as the Sultansuyu (Fig. 02) and the Beyler Deresi (Fig. S4a), to create the modern dissected landscape in the Malatya Basin interior. Fluvial deposits that post-date the start of this incision are not shown. Except where other environments are indicated, the stacked succession is lacustrine or low-energy fluvial, the proportions of both types of input varying laterally and over time, as indicated by the lithologies. The Mamaar volcanics, depicted, in the central Malatya Basin are equivalent, according to Kaymakcı et al. (2006), to the Yamadağ volcanics farther north (Fig. 2 in the main text). The latter volcanism is Middle Miocene, given K-Ar dates of 18.7±0.5, 16.8±0.5 and 14.1±0.4 Ma (Leo et al., 1974), and of 15.9±0.4 and 15.2±0.5 Ma (Arger et al., 2000). As noted in the main text, this K-Ar interpretation and the pollen evidence (Önal, 1995, 1997) for a Middle Miocene age for the Parçikan Formation is contradicted by mammalian biostratigraphic evidence from Kaymakcı et al. (2006), which requires the lower part of this deposit (Fig. S3) to be no older than the early Late Miocene. Kaymakcı et al. (2006) suggested using the name Sultansuyu Formation for terrace deposits of the Sultansuyu, Tohma and Kuru rivers that are inset into the stacked sequence of the Malatya Basin. However, this would be confusing, as the same name is already in use for older deposits in the region, as illustrated. Regarding the chronology, Önal (1995, 1997) proposed that the whole sequence above the Küseyin Formation is Middle Miocene, but provided no age-control above the Upper Lignite, which could be latest Middle Miocene. Kaymakcı et al. (2006) suggested that the low-energy sediments above the stratigraphic level of the Mamaar / Yamadağ volcanics, including the Upper Lignite, are Late Miocene, and the overlying coarse fluvial clastics are Early to Middle Pliocene, the latter age assignment based on a correlation with the lacustrine deposits at Sürsürü near Elazığ (see text and Fig. S3). However, such a correlation seems most unlikely, as the lithologies in the two localities are very different. We tentatively infer that the deposits of the Beyler Deresi Formation are Late Pliocene, having aggraded after the Mid-Pliocene climatic optimum but before the regionl increase in uplift rates at ~2 Ma (see text).

Figure S3. Schematic north-south cross-section through the Malatya Basin, based on Fig. 4 of Önal (1995), with additional information from Önal (1995, 1997), Kaymakçı et al. (2006) and this study. See Fig. 2 in the main text for location; named localities are projected onto this section line from either side. Sediment thicknesses are constrained in the north (from Boyaca northward) by outcrop evidence and in the south (beneath the Beyler Deresi Formation) by boreholes for lignite prospecting. In the centre of the basin they are not constrained; as noted in the text, the seismic reflection evidence by Kaymakçı et al. (2006) (line 4 in their Fig. 11) suggests that the succession is much thicker here than is shown in this illustration. Much of this thickness consists of deposits of the Boyaca Formation, the base of which is thus well below the level of incision by the Kuru and Tohma rivers. Geometry of sedimentary fill has been drawn below a horizontal datum linking the tops of the Arkaç Dağ fluvial deposits and the Beyler Deresi Formation.To achieve this, folding across the Aydınlar anticline has been restored; the extent of this folding can be judged from the lateral variation, depicted, in the extent to which the basin stratigraphy has been locally eroded. Dashed lines indicate, schematically, the estimated extents of erosion of the Sultansuyu, Boyaca, and Parçikan formations above the highest points in the present-day landscape. Note the much greater extent of this erosion in the north than in the south, consistent with the much greater incision by the Kuru river below the Arkaç Dağ deposits (~350 m) compared with that by the Beyler Deresi below the top of the Beyler Deresi Formation (~70 m).

Figure S4. Malatya Basin field photos. **(a)** View northward, looking down the Beyler Deresi valley from [DC 31090 43362], ~5 km west of Malatya. The view illustrates coarse, poorly-sorted but well-stratified fluvial conglomerate of the Beyler Deresi Formation, which has been incised by ~70 m (locally, from ~900 m to ~830 m a.s.l.) to create the modern dissected fluvial landscape. Note the flat upper surface of the conglomerate, the top of the stacked sequence in the Malatya Basin, in the interfluves on both sides of the young river gorge. **(b)** View of the west face of the cutting on highway 875 (Malatya–Keban) at [DC 37666 76675] in the central Malatya Basin, showing the lacustrine sequence (clay, silt, lignite, etc.) of the Parçikan Formation, mentioned in the text, tilted steeply to the south. The stratigraphic section illustrated is ~10 m thick.

Figure S5. Field photos illustrating the Ovacık Fault near Başpınar (Fig. 2 in the main text). See Westaway and Arger (2001) for detailed maps of this area. **(a)** View NNE from [DD 75952 38069], looking obliquely across the line of the Ovacık Fault (marked) that follows the gulley in the foreground (~500 m away). The left-lateral component of slip on this fault has locally juxtaposed (?) Miocene evaporites on the far side against the Keban metamorphics on the near side. The summit in the upper left centre of the field of view is Doymuş Tepe (2542 m a.s.l.; c. [DD 778 450]; ~ 7 km away), in the upper part of the Keban metamorphics north of the fault. Behind and left of it is the higher summit of Ziyaret Tepe (3147 m a.s.l.; c. [DD 763 484]; ~10 km away), one of the highest peaks in the Munzur range. This is in the unmetamorphosed Mesozoic limestone of the Munzur Group, which was thrust southward onto the Keban Group during the mid-Cenozoic phase of crustal shortening. Careful inspection reveals the northnorthwestward back-tilting of the stratigraphy of the Munzur Group, consistent with a component of downthrow to the SSE during slip on the Ovacık Fault. **(b)** View towards S80°W from [DD 77048 36981], ~1400 m a.s.l., looking along the reach of the River Euphrates that has become offset left-laterally by ~8 km by this fault. The gorge flanks rise to ~1700 m a.s.l. on the left and ~1600 m on the right. This gorge, cut into the Keban group metamorphics (typically, calcschist), reaches down a few tens of metres below the surface of the Keban reservoir at ~850 m a.s.l. The ~2 km width of this gorge makes it difficult to estimate piercing points for the MOFZ slip to high precision.


(a)

(b)

(c)
Figure S1

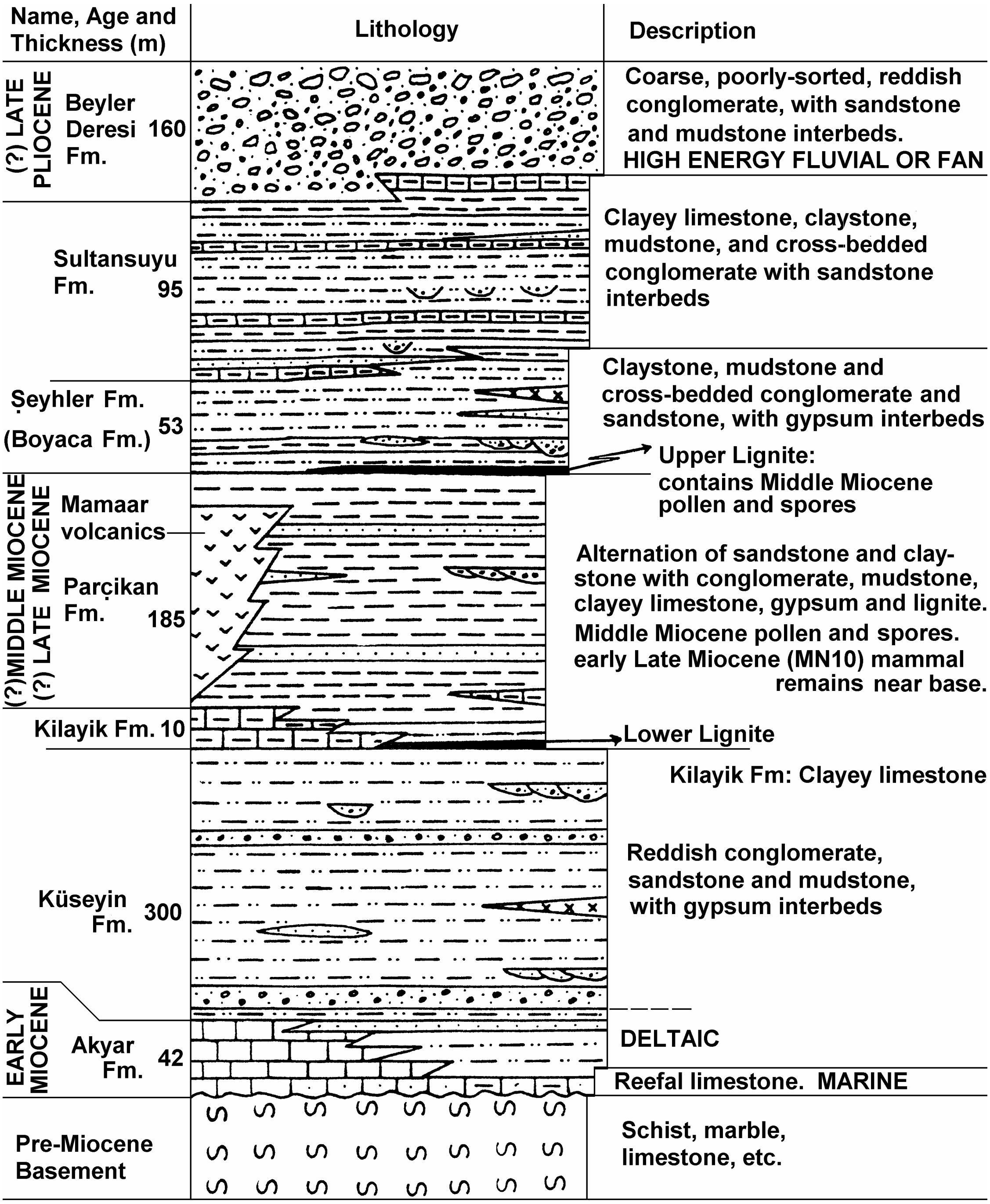
Name, Age and Thickness (m)
Lithology
Description
(?) LATE PLIOCENE
Beyler Deresi Fm. 160
Coarse, poorly-sorted, reddish conglomerate, with sandstone and mudstone interbeds.
HIGH ENERGY FLUVIAL OR FAN
Sultansuyu Fm. 95
Clayey limestone, claystone, mudstone, and cross-bedded conglomerate with sandstone interbeds
Şeyhler Fm. (Boyaca Fm.) 53
Claystone, mudstone and cross-bedded conglomerate and sandstone, with gypsum interbeds
Upper Lignite: contains Middle Miocene pollen and spores
(?)MIDDLE MIOCENE
(?) LATE MIOCENE
Mamaar volcanics
Parçikan Fm. 185
Alternation of sandstone and claystone with conglomerate, mudstone, clayey limestone, gypsum and lignite. Middle Miocene pollen and spores. early Late Miocene (MN10) mammal remains near base.
Kilayik Fm. 10
Lower Lignite
Kilayik Fm: Clayey limestone
Küseyin Fm. 300
Reddish conglomerate, sandstone and mudstone, with gypsum interbeds
EARLY MIOCENE
DELTAIC
Akyar Fm. 42
Reefal limestone. MARINE
Pre-Miocene Basement
Schist, marble, limestone, etc.

Figure S2

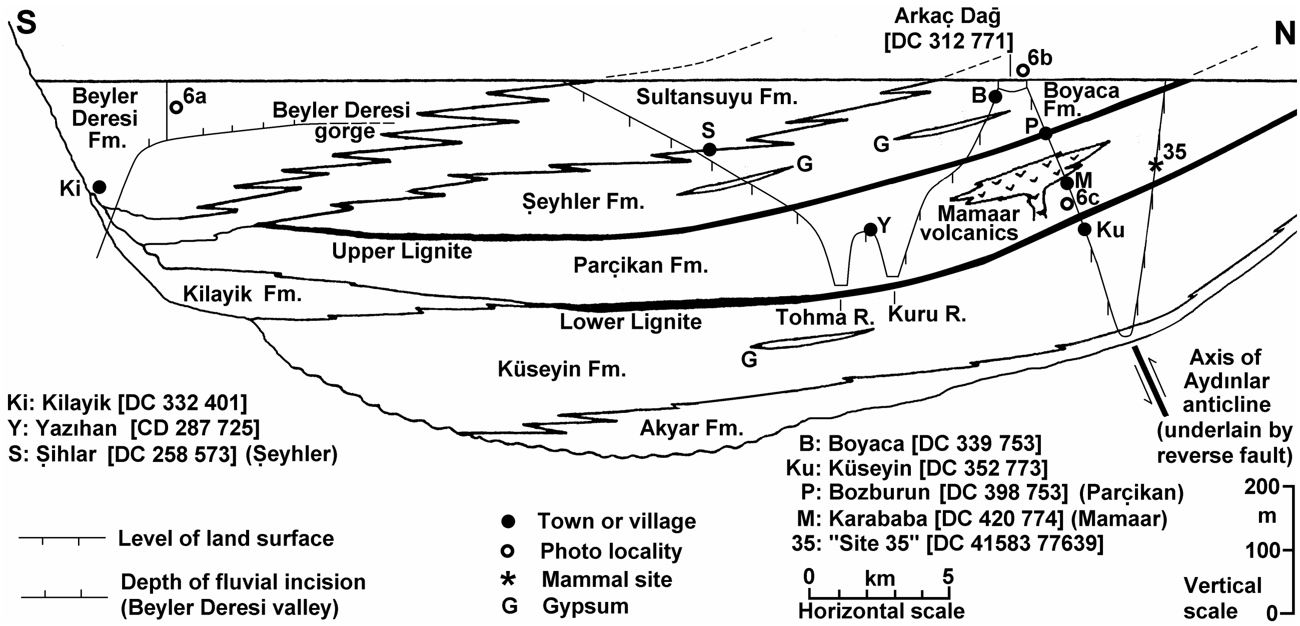
S
N
Arkaç Dağ
[DC 312 771]
6b
Beyler
Deresi
Fm.
6a
Beyler Deresi
gorge
Sultansuyu Fm.
B
Boyaca
Fm.
P
S
G
G
35
M
6c
Ki
Şeyhler Fm.
Mamaar
volcanics
Y
Ku
Upper Lignite
Parçikan Fm.
Kilayik Fm.
Lower Lignite
Tohma R.
Kuru R.
G
Küseyin Fm.
Axis of
Aydınlar
anticline
(underlain by
reverse fault)
Ki: Kilayik [DC 332 401]
Y: Yazıhan [CD 287 725]
S: Şihlar [DC 258 573] (Şeyhler)
Akyar Fm.
B: Boyaca [DC 339 753]
Ku: Küseyin [DC 352 773]
P: Bozburun [DC 398 753] (Parçikan)
M: Karababa [DC 420 774] (Mamaar)
35: "Site 35" [DC 41583 77639]
200
m
100
Vertical
scale
0
Level of land surface
Depth of fluvial incision
(Beyler Deresi valley)
Town or village
Photo locality
Mammal site
G Gypsum
0 km 5
Horizontal scale
Figure S3

(a)

(b)

Figure S4


(a)

(b)
Figure S5